Is Bismuth(III) able to inhibit the activity of urease? Puzzling results in the quest for soluble urease complexes for agrochemical and medicinal applications

Laura Contini,[a] Arundhati Paul,[b] Luca Mazzei,[b] Stefano Ciurli,[b,*] Davide Roncarati,[c,*] Dario Braga,[a] Fabrizia Grepioni[a,*]

[a] Department of Chemistry "G. Ciamician", University of Bologna, Via Selmi 2, 40126 Bologna, Italy

[b] Laboratory of Bioinorganic Chemistry, Department of Pharmacy and Biotechnology (FaBiT), University of Bologna, Viale Giuseppe Fanin 40, Bologna I-40127, Italy

[c] Department of Pharmacy and Biotechnology (FaBiT), University of Bologna, Via Selmi 3, 40126 Bologna, Italy

Electronic Supplementary Information (10 pages)

1. Powder X-ray diffraction

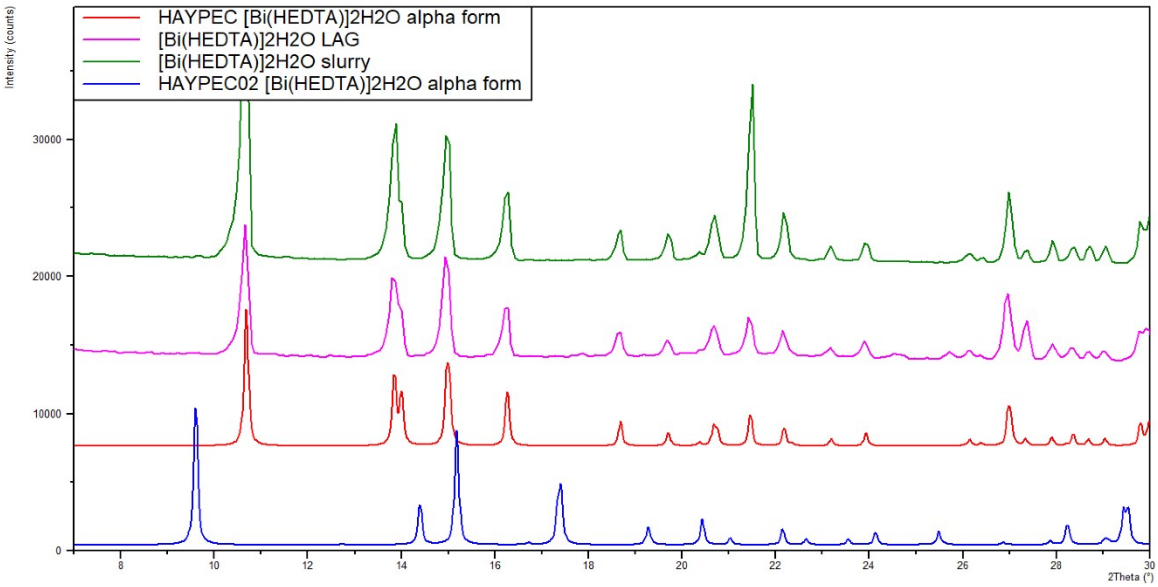

Figure ESI 1: Comparison between the experimental PXRD patterns for [Bi(HEDTA)]·2H_2O (**1**) obtained via LAG (pink) and slurry (green) and the calculated ones for the β (red) and α (blue) forms.

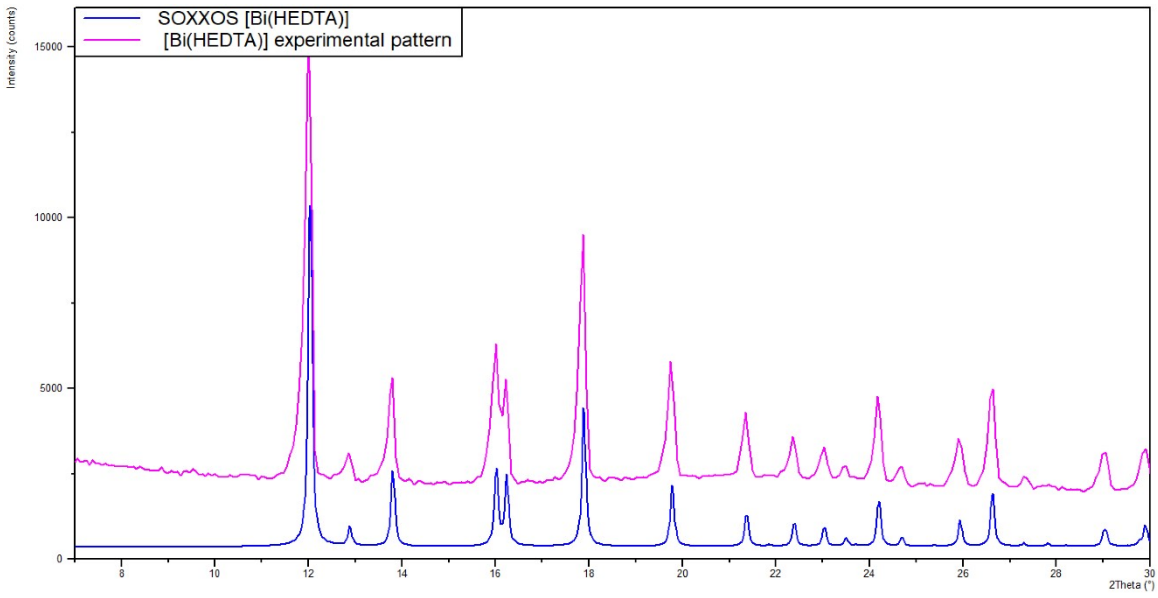

Figure ESI 2: Comparison between the experimental PXRD of [Bi(HEDTA)] (**2**) obtained via heating of the dehydrated form (pink) and the calculated one of [Bi(Hedta)] (blue)

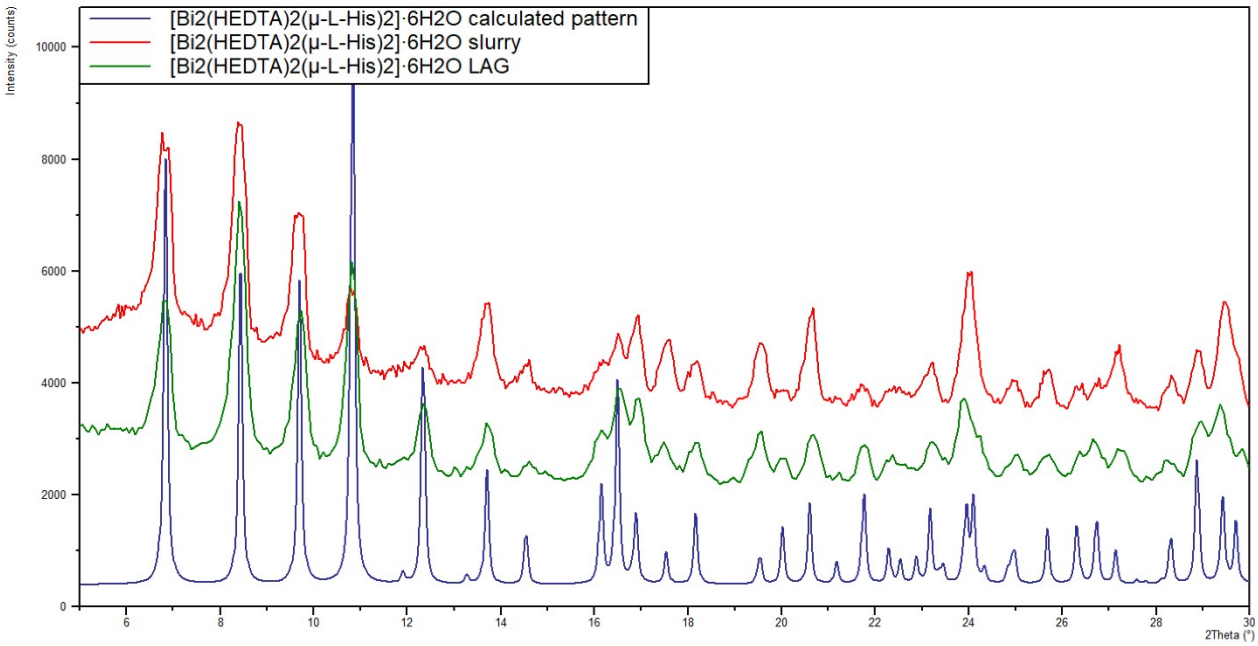

Figure ESI 3: Comparison between the experimental PXRD patterns for $[Bi_2(HEDTA)_2(\mu\text{-L-His})_2]\cdot 6H_2O$ (**4**) obtained via slurry (red) and LAG (green) and the calculated one (blue).

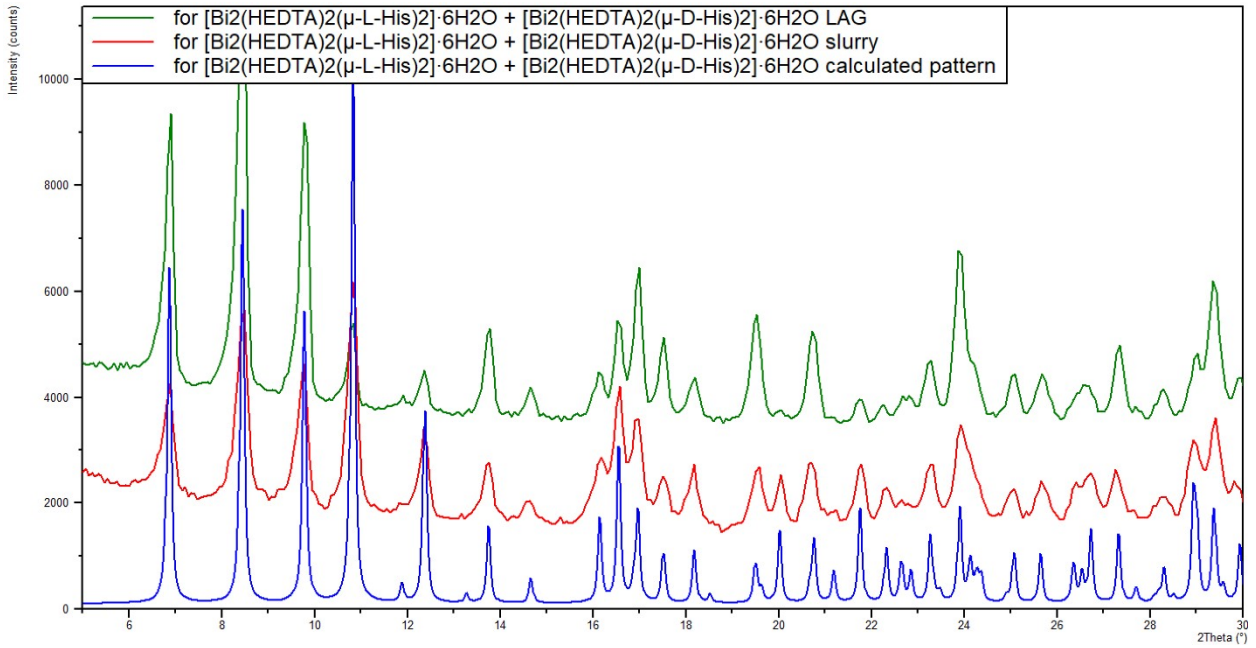

Figure ESI 4: Comparison between the experimental PXRD patterns for the conglomerate $[Bi_2(HEDTA)_2(\mu\text{-L-His})_2]\cdot 6H_2O$ + $[Bi_2(HEDTA)_2(\mu\text{-L-His})_2]\cdot 6H_2O$ (**3**) obtained via slurry (red) and LAG (green) and the calculated one (blue).

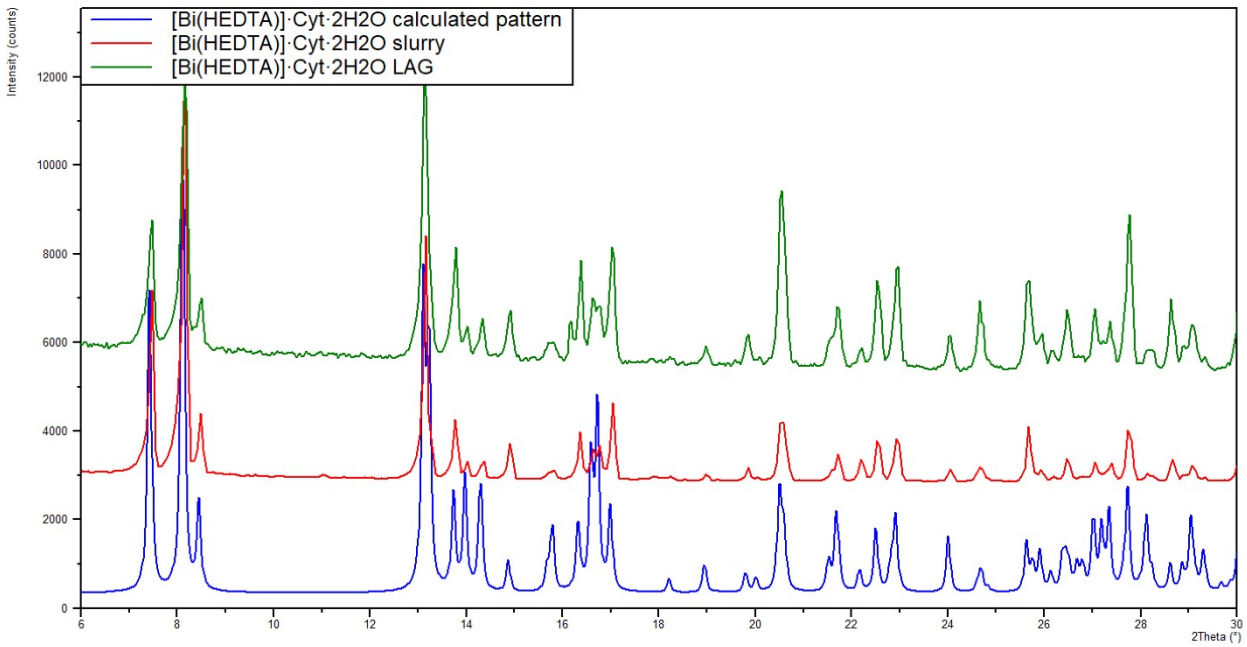

Figure ESI 5: Comparison between the experimental PXRD patterns for [Bi(HEDTA)]·Cyt·2H_2O (**5**) obtained via slurry (red) and LAG (green) and the calculated one (blue).

2. Crystal data and Rietveld refinements

Table ESI 1: Cell parameters and Rwp values at 293K for the conglomerate [Bi_2(HEDTA)$_2$(μ-L-His)$_2$]·6H_2O + [Bi_2(HEDTA)$_2$(μ-D-His)$_2$]·6H_2O (**3**), [Bi_2(HEDTA)$_2$(μ-L-His)$_2$]·6H_2O (**4**) and [Bi(HEDTA)]·Cyt·2H_2O (**5**) (all structures from powder data).

	[Bi_2(HEDTA)$_2$(μ-L-His)$_2$]·6H_2O + [Bi_2(HEDTA)$_2$(μ-D-His)$_2$]·6H_2O (**3**)[a]	[Bi_2(HEDTA)$_2$(μ-L-His)$_2$]·6H_2O (**4**)[b]	[Bi(HEDTA)]·Cyt·2H_2O (**5**)[c]
Chemical formula	C16 H28 Bi N5 O13	C16 H28 Bi N5 O13	C14 H22 Bi N5 O11
Formula weight (g·mol^{-1})	707.399	707.399	645.332
Crystal system	Monoclinic	Monoclinic	Triclinic
Space group	C2	C2	P-1
a (Å)	21.358(4)	21.395(5)	13.0539(12)
b (Å)	8.8650(16)	8.855(2)	11.9390(11)
c (Å)	13.125(2)	13.191(3)	6.8072(6)
α (°)	90.000	90.000	96.318(3)
β (°)	101.303(4)	101.901(5)	96.953(3)
γ (°)	90.000	90.000	113.171(2)
V (Å^3)	2436.8(8)	2445.2(10)	953.59(16)
Z, *Z'*	4,1	4,1	2, 1
Rwp %	9.792	10.246	8.161

[a] Conglomerate: crystal data are reported here with the only purpose of confirming the obtainment of a conglomerate. [b] CCDC number 2340274. [c] CCDC number 2340273.

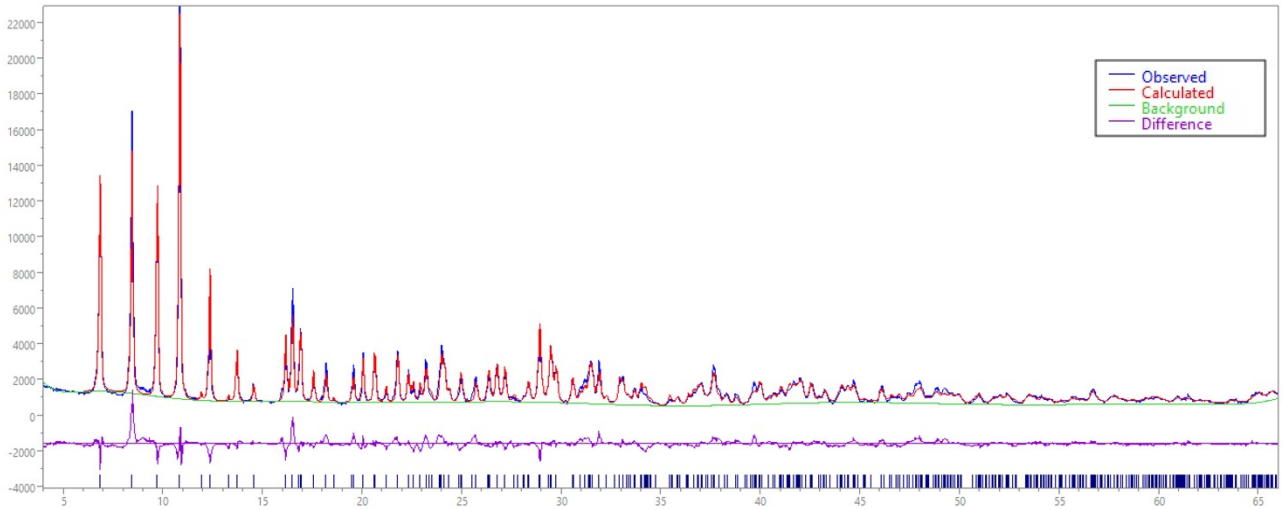

Figure ESI 6: Rietveld refinement. Experimental (blue curve), calculated (red curve) background (green curve), and difference (purple curve) powder patterns for $[Bi_2(HEDTA)_2(\mu\text{-L-His})_2]\cdot 6H_2O$ (**4**).

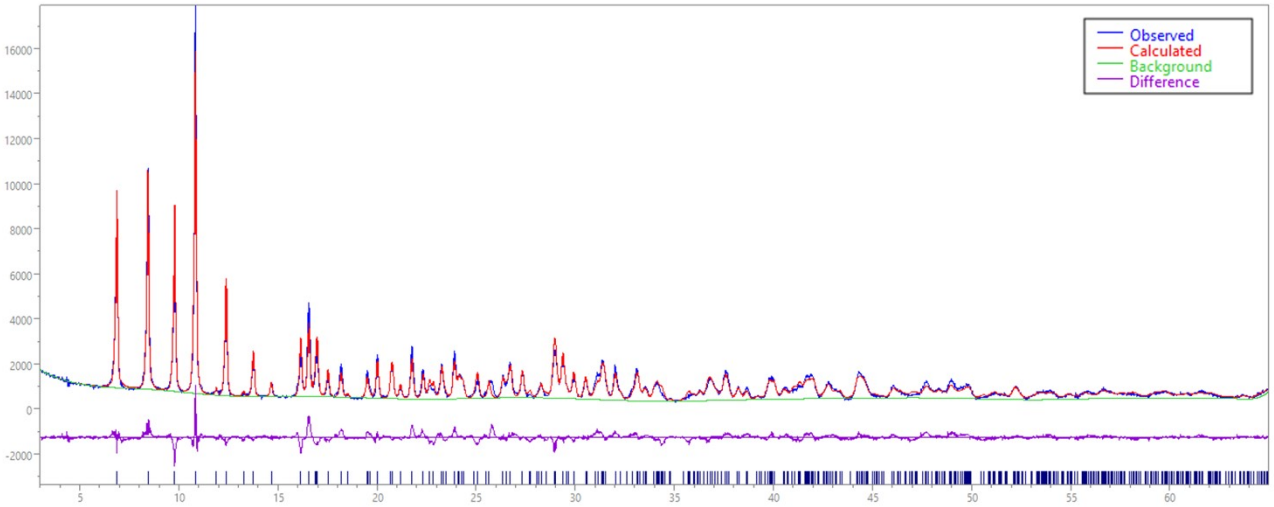

Figure ESI 7: Rietveld refinement. Experimental (blue curve), calculated (red curve), background (green curve), and difference (purple curve) powder patterns for the conglomerate $[Bi_2(HEDTA)_2(\mu\text{-L-His})_2]\cdot 6H_2O$ + $[Bi_2(HEDTA)_2(\mu\text{-D-His})_2]\cdot 6H_2O$ (**3**)

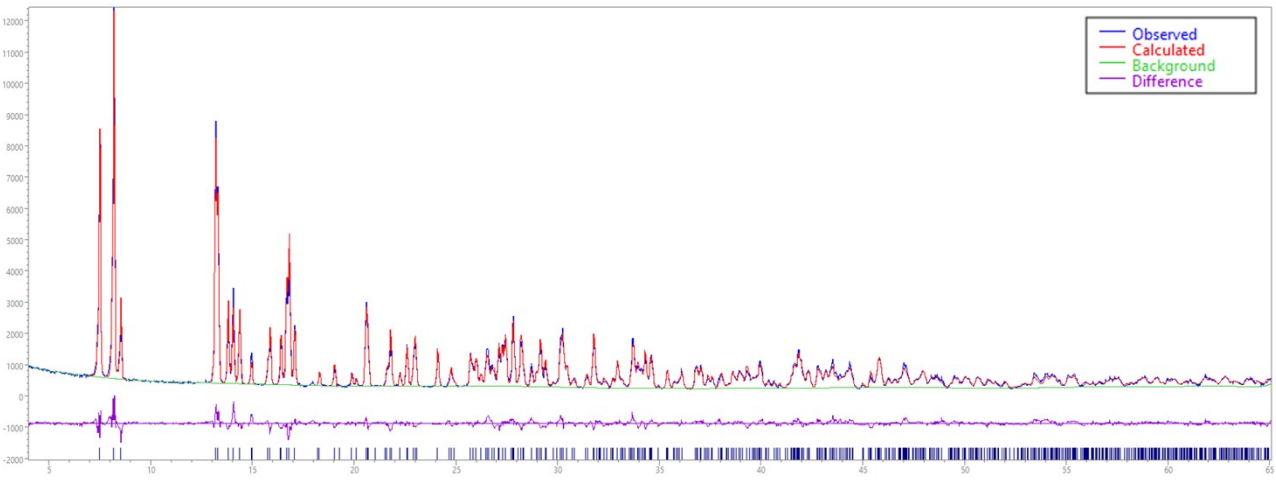

Figure ESI 8: Rietveld refinement. Experimental (blue curve), calculated (red curve) background (green curve), and difference (purple curve) powder patterns for [Bi(HEDTA)]·Cyt·2H_2O (**5**)

3. DSC and TGA

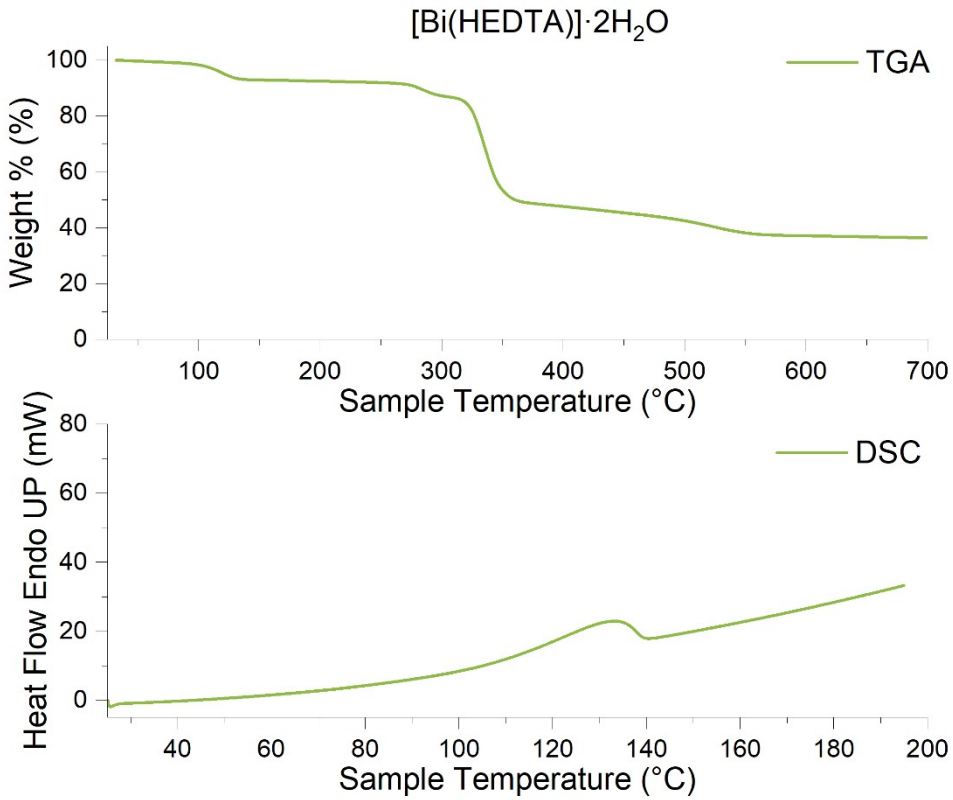

Figure ESI 9: TGA and DSC traces for [Bi(HEDTA)]·2H_2O (**1**)

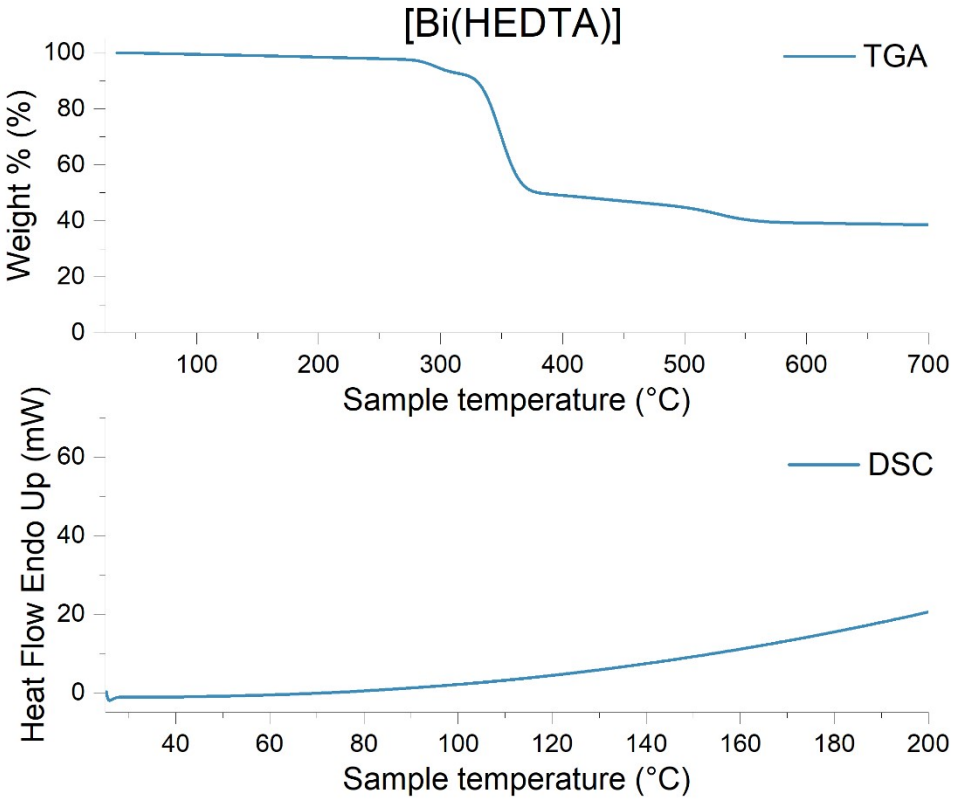

Figure ESI 10: TGA and DSC traces for [Bi(HEDTA)] (**2**)

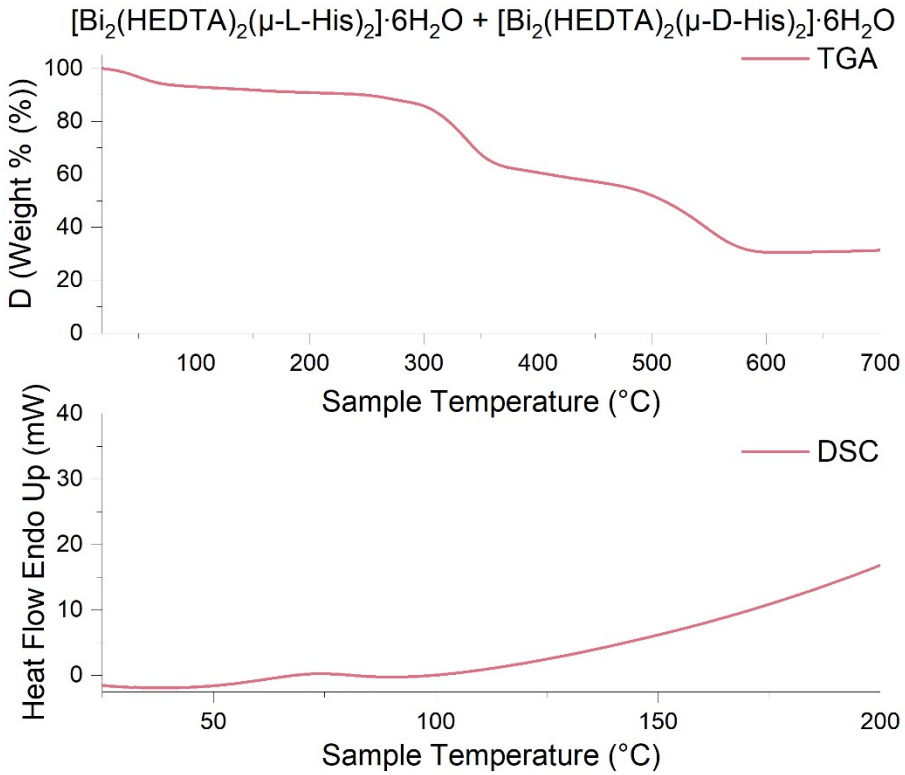

Figure ESI 11: TGA and DSC traces for the conglomerate $[Bi_2(HEDTA)_2(\mu\text{-L-His})_2]\cdot 6H_2O$ + $[Bi_2(HEDTA)_2(\mu\text{-D-His})_2]\cdot 6H_2O$ (**3**)

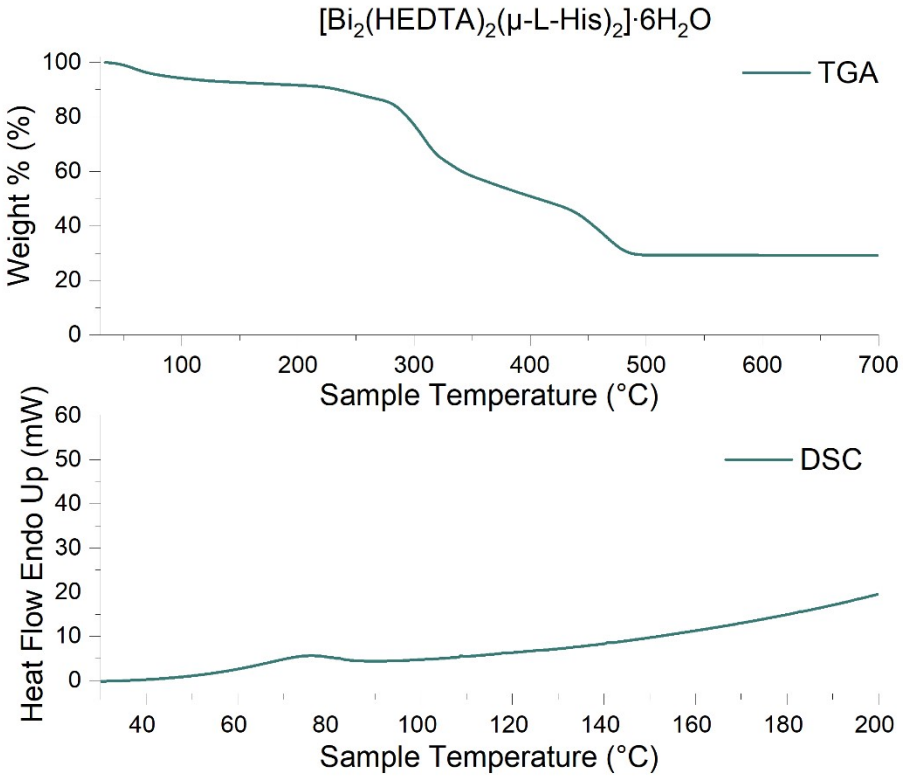

Figure ESI 12: TGA and DSC traces for $[Bi_2(HEDTA)_2(\mu\text{-L-His})_2]\cdot 6H_2O$ (**4**)

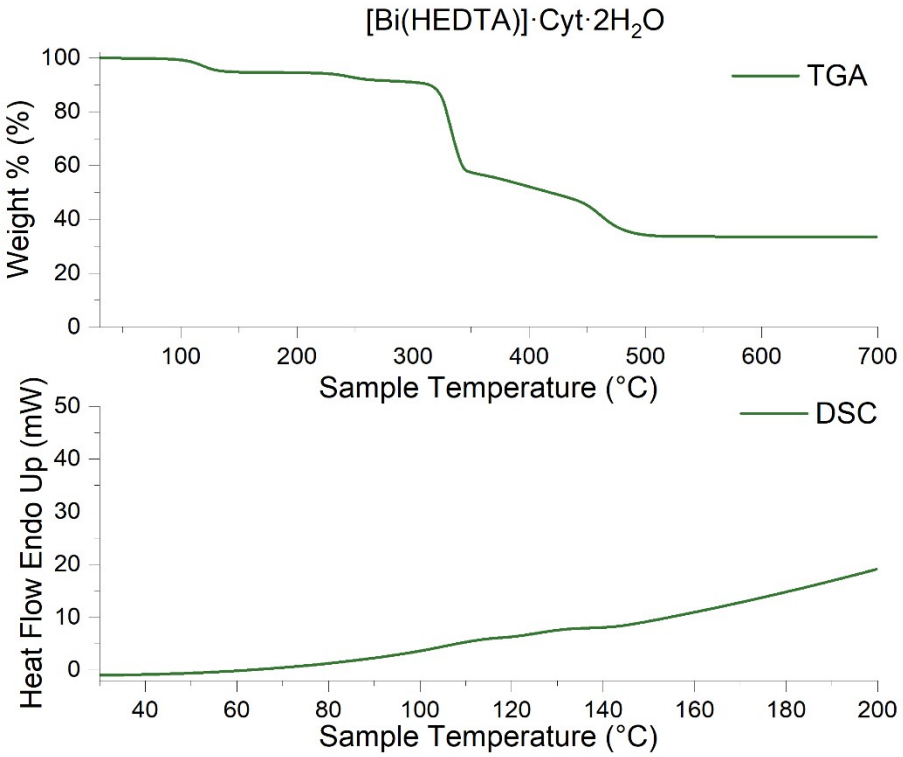

Figure ESI 13. TGA and DSC traces for [Bi(HEDTA)]·Cyt·2H_2O (**5**)

4. ^{1}H NMR

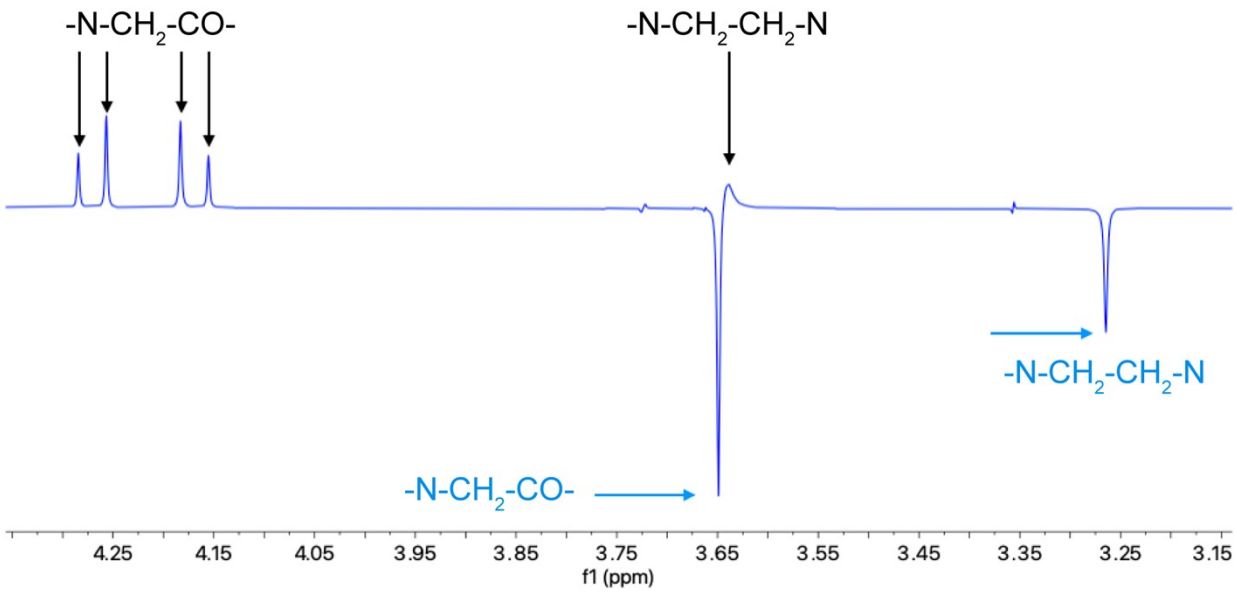

Figure ESI 14. Difference ^{1}H NMR spectrum of 1 mM [Bi(HEDTA)]·2H_2O (**1**) *vs.* 1 mM H_4EDTA, recorded in 50 mM phosphate buffer in D_2O at pD 7.5. The spectra were recorded on a Bruker Ascend 600 NMR spectrometer equipped with an Advance Neo console and a PRODIGY cryoprobe, operating at 599.74 MHz, using the "s2pul" pulse sequence. Spectral width: 16 ppm; number of scans: 120; acquisition time: 2.99 s; repetition delay: 1 s. The experiments were carried out at 298 K. Data were processed using the MestreNova software version 15. The spectrum of the free ligand shows two singlets at δ = 3.26 and 3.65 ppm (cyan), arising from the four acetate-methylene protons and the two backbone methylene groups, respectively. The spectrum of the Bi(III) complex shows signals of [Bi(HEDTA)] (black) similar to those previously reported for ^{1}H NMR spectra of EDTA complexes with different divalent metal ions.[1] In the case of the Bi(III) complex, both the methylene protons in the N-CH_2-CH_2-N- groups (appearing as a broadened singlet at δ = 3.64 ppm, indicative of a fluxional conformation behaviour), and the four acetate-methylene geminal protons in the N-CH_2-CO- group (appearing as sharp doublets in the δ = 4.16 – 4.28 ppm range) are shifted more downfield with respect to the free ligand as compared to the analogous chemical shifts of divalent metal ions,[1] due to the presence of the higher charge on the bound Bi(III). Two groups of acetate methylene protons are observed at 4.17 and 4.27 ppm; within each group, the two methylene protons have different chemical environments due to restricted rotation resulting in two different configurations, Δ and Λ.[2] The two 2J (^{1}H-^{1}H) coupling constants are 16.64 and 16.65 Hz.

5. Antimicrobial activity tests

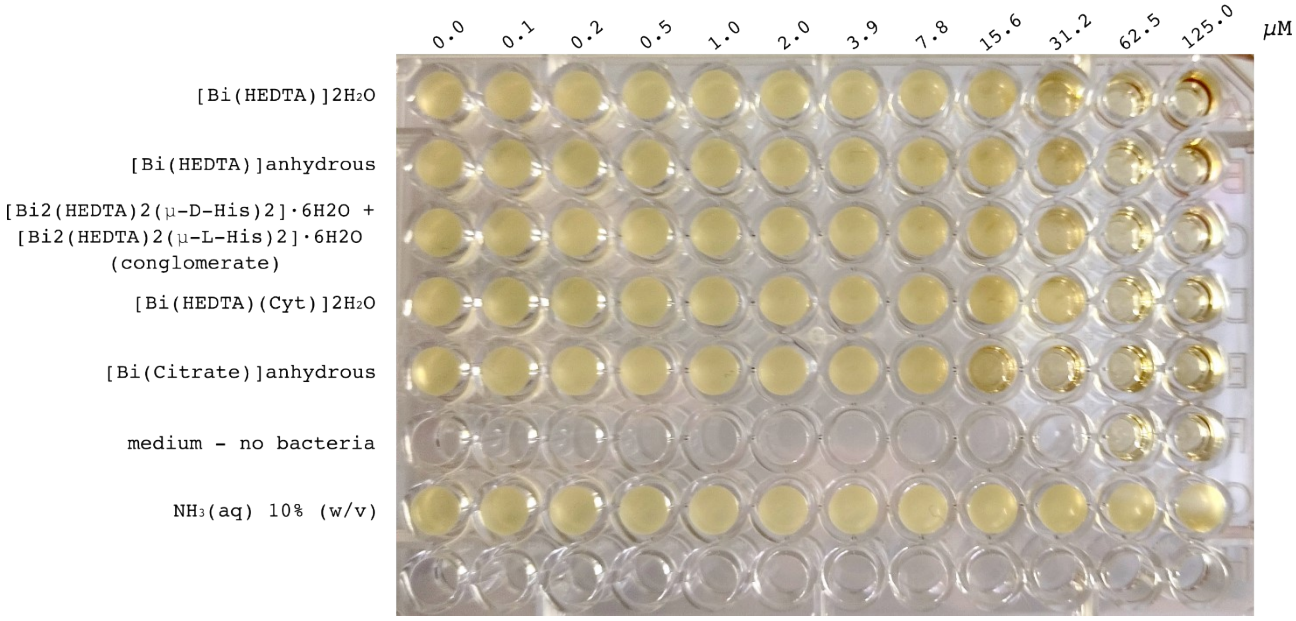

Figure ESI 15: Minimal inhibitory concentration (MIC) assay for the antimicrobial activity of Bismuth-containing compounds on *H. pylori* G27 liquid culture.

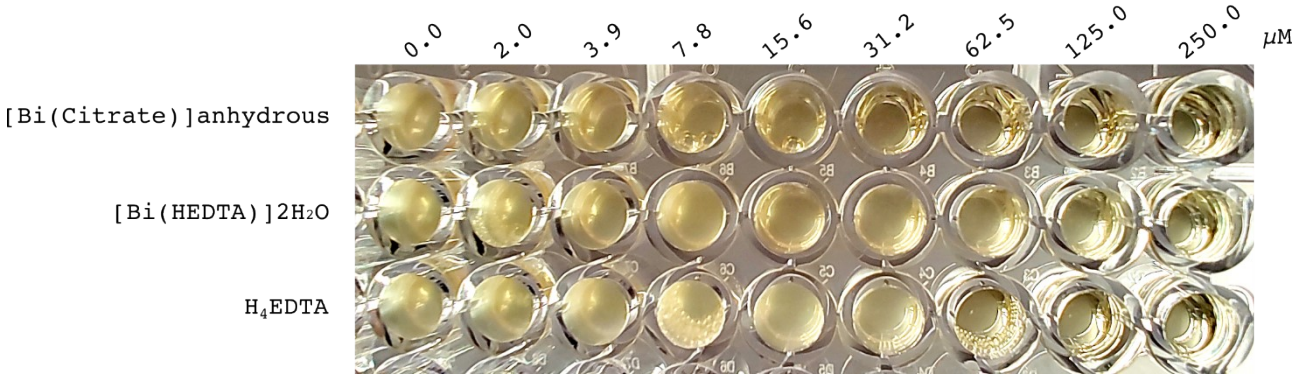

Figure ESI 16: Minimal inhibitory concentration (MIC) assay for the antimicrobial activity of Bismuth-containing compounds on *H. pylori* G27 liquid culture: comparison between [Bi(citrate)], [Bi(HEDTA)]·2H_2O and H_4EDTA.

6. Bibliography

1 E. Hafer, U. Holzgrabe, K. Kraus, K. Adams, J. M. Hook and B. Diehl, *Magnetic Resonance in Chemistry*, 2020, **58**, 653–665.
2 M. C. Gennaro, P. Mirti and C. Casalino, *Polyhedron*, 1983, **2**, 13–18.